# Microwave spin-torque excitation in a template-synthesized nanomagnet

N. Biziere, E. Murè, and J.-Ph. Ansermet
*Institut de Physique des Nanostructures, Ecole Polytechnique Fédérale de Lausanne (EPFL), Station 3, CH-1015 Lausanne, Switzerland*
(Received 7 July 2008; revised manuscript received 17 October 2008; published 20 January 2009)

A microwave-compatible lithography-free process is shown to allow the electrical contact of a single nanometric spin valve grown by template synthesis. The complex spin dynamics of a single nanomagnet is revealed by resonant microwave current excitations, detected electrically in the $V_{dc}$ and second-harmonic voltages. The uniform modes are attributed to spin transfer torque effects, whereas the effect of oersted field may play a role in exciting the nonuniform modes.

DOI: 10.1103/PhysRevB.79.012404 PACS number(s): 76.50.+g, 72.25.Ba, 73.43.Fj

The effect of a spin-polarized current on magnetization dynamics, shown theoretically[1,2] then verified experimentally,[3–5] requires current densities on the order of $10^7$ A/cm$^2$. As a consequence, it can only be observed and used with currents confined to nanoscale geometries. This effect, known as the spin transfer torque (STT), opens up very attractive prospects for microwave devices in wireless communications and data storage technology.[6,7] Individual structures are produced by state-of-the-art nanoscale lithography and the high-frequency range of these spintronic devices implies electrical connections by transmission lines. DC currents (dc) through spin valves (SV) have been shown to induce microwave oscillations[8] so there is a keen interest in ways to produce SVs in series.[9]

In this Brief Report, a lithography-free process has been developed to grow sub-100 nm SV pillars connected in current perpendicular to plane (CPP) configuration. The microwave performance is demonstrated by detecting several ferromagnetic resonance modes of our device excited by resonant STT. This experiment relies on the possibility for a resonant current passing through the nanowire to excite fundamental magnetic modes of the system, leading to a change in the static voltage across the structure. To our knowledge few studies of ac excitation in spin transfer phenomena have been carried out[10–14] although these may offer new insight into the physics of STT, and none of them used embedded nanowires. As the technique we used, template synthesis, is very promising for applications with the possibility of integrating multiple resonators in series, one needs a better understanding of the spin dynamics in individual nanostructures produced by this method.

A critical issue for these STT experiments is the fabrication of magnetic multilayers of very small cross sections (typically around 100 nm in diameter). Our technique uses the electrodeposition[15] of nanopillars in a 6-$\mu$m-thick ion track etched polycarbonate commercial membrane. First we evaporate a gold film of a few microns in thickness on one side of the membrane. This acts as the bottom electrical contact to the pillar. This metallized side of the membrane is then placed on top of a metallic pin designed to fit a female subminiature version A (SMA) connector. The mechanical contact between the membrane and the pin is ensured by a Teflon cap screwed onto the pin [Fig. 1(a)]. The system pin/membrane is then immersed in a cobalt/copper bath for electrodeposition of a $Cu_{(1\ \mu m)}/Co_{(40\ nm)}/Cu_{(5\ nm)}/Co_{(5\ nm)}/Cu_{(5\ \mu m)}$ stack. In the following, the thin and thick Co layers will be referred to for convenience as the soft (SL) and hard (HL) layers, respectively. The pores of the membrane have a diameter of about 80 nm. The plating of the nanowires is extended so as to form at the surface of the membrane Cu bumps of a few microns in diameter. The use of a single bath induces the presence of about 15% of Cu in the deposited Co and yields a smaller value of $\mu_0 M_s$ ($\simeq$1.15 T) than that of bulk Co (1.6 T). More details about the electrodeposition procedure can be found elsewhere.[16]

The SMA connector with the pin and the filled membrane is closed by a metallic cap that supports a screw on which a gold wire of a few microns in diameter is welded. We drag the gold wire over the surface of the membrane until it touches a Cu bump and thus achieves the top electrical contact to one nanostructure. A small fraction of the pores is filled during electrodeposition so only one or two nanowires are electrically connected by the gold wire [Fig. 1(a)]. Others, also working with templates, have used a nanoindenter to ensure single contact to similar nanostructures.[17]

When dealing with STT effects, one needs to know the current density passing through the nanowire. Here we calibrate the rf current injected in the sample by monitoring the joule heating detected as a change in resistance. First, a $dV/dI$ measurement is performed with a dc in order to calibrate the change in resistance as a function of the current due to joule heating. Then the sample resistance is monitored with a small dc while a large rf current of constant power is injected simultaneously. The frequency $\omega/2\pi$ is scanned from 2 to 18 GHz. The increase in resistance due to the rf current is then compared to that obtained by the dc measurements to estimate the rf current amplitude as function of $\omega$.

The ferromagnetic resonance (FMR) of the spin valve is detected as its electrical response to an ac in the microwave range. Indeed, provided that the SL and HL magnetizations present a relative angle at equilibrium $\theta \neq 0$ with respect to one another, the current induces the precession of the magnetization when its frequency $\omega_{ac}/2\pi$ corresponds to the FMR frequency. Then, because of the giant magnetoresistance (GMR) effect, the voltage $V(t)$ across the spin valve given by the product $R(t)I(t)$ contains two equal amplitude signals at zero frequency ($V_{dc}$) and at the second harmonic ($V_{2\omega}$).[18] As a first approximation the $V_{dc}$ voltage can be expressed as $\frac{1}{4}\Delta R I_{rf} \sin\theta \sin\psi$, where $\psi$ is the angle of precession and $\Delta R$ is the difference of resistance between the antiparallel and parallel states.

 ©2009 The American Physical Society

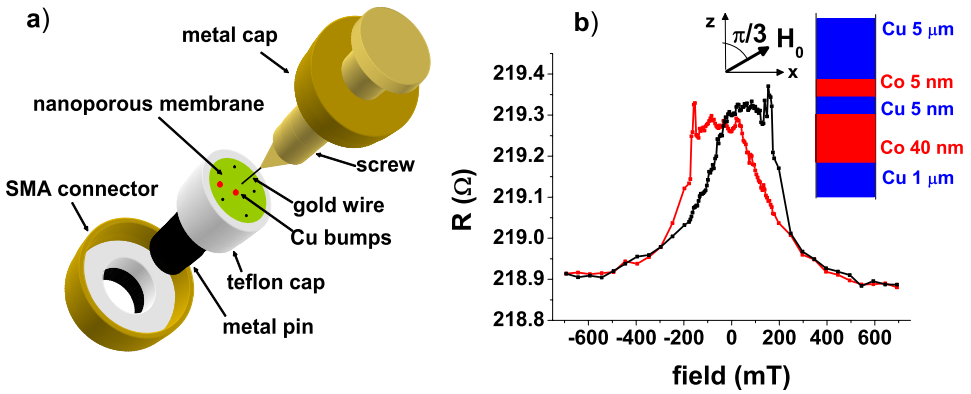


FIG. 1. (Color online) (a) Blown up view of the connector assembly fitted with a nanoporous membrane and gold wire contact. (b) Magnetoresistance cycle as a function of the applied field $H_0$. The field sweeps up (black) and down (red) from −700 to +700 mT. The inset shows the structure of the spin valve.

The quality of the connected SV is assessed by measuring the GMR as a function of the external static magnetic field $H_0$ applied parallel to the membrane surface [Fig. 1(b)]. The field is then at an angle of about $\pi/3$ rad relative to the pore axis, owing to the average orientation of the pores in the membrane.[19] The asymmetry of the GMR cycle reflects the competition between $H_0$ and $H_{\text{bias}}$, the dipolar field created by the HL on the SL. The average resistance of 219 Ω is dominated by the length of the nanowire, which is orders of magnitude longer than the spin valve itself. The capacity of the technique to perform dc STT experiments is demonstrated by the presence of peaks in the $dV/dI$ measurement [Fig. 2(d)]. In our setup, a positive current corresponds to electrons flowing from the SL to the HL.

Figures 2(a) and 2(b) present the static voltage response as a function of the frequency of the injected current, measured at different values of $H_0$. The external magnetic field is scanned from −700 to 700 mT. The measurements have been performed with an amplitude of the injected rf current of about 450 μA, roughly constant between 2 and 10 GHz, and then decreasing to 300 μA at 18 GHz. The second-harmonic detection [Fig. 2(c)] shows that our setup allows the detection of very small signals at microwave frequencies. In this experiment, we averaged 1000 scans to get sufficient signal-to-noise ratio. Since both signals give the same information about the physics, we collected mostly $V_{\text{dc}}$ spectra as they are easier to detect. From the $V_{\text{dc}}$ amplitude, we evaluate the angle of precession to be $\leq 10°$ for each FMR excitation.

Close to the saturated regime of both layers [$|H_0| > 290$ mT, Fig. 2(a)], the $V_{\text{dc}}$ spectra present a single peak whereas in the low-field range [$-150 < H_0 < 150$ mT, Fig. 2(b)], multiple peaks or dips are observed. We report the evolution of the frequency of these modes as a function of the external field in Fig. 3. We note that resonances are observed until the SL and HL are completely saturated in the direction of $H_0$, a saturation that can also be seen in the GMR curve. The vanishing excitation is consistent with the $\sin\theta$ dependence of the $V_{\text{dc}}$ signal.

In order to explain the spectra, we first calculate the fundamental (uniform) FMR mode of each layer considered as a macrospin, as a function of the applied field $H_0$. This is achieved by solving the general equation[20] (in spherical coordinates):

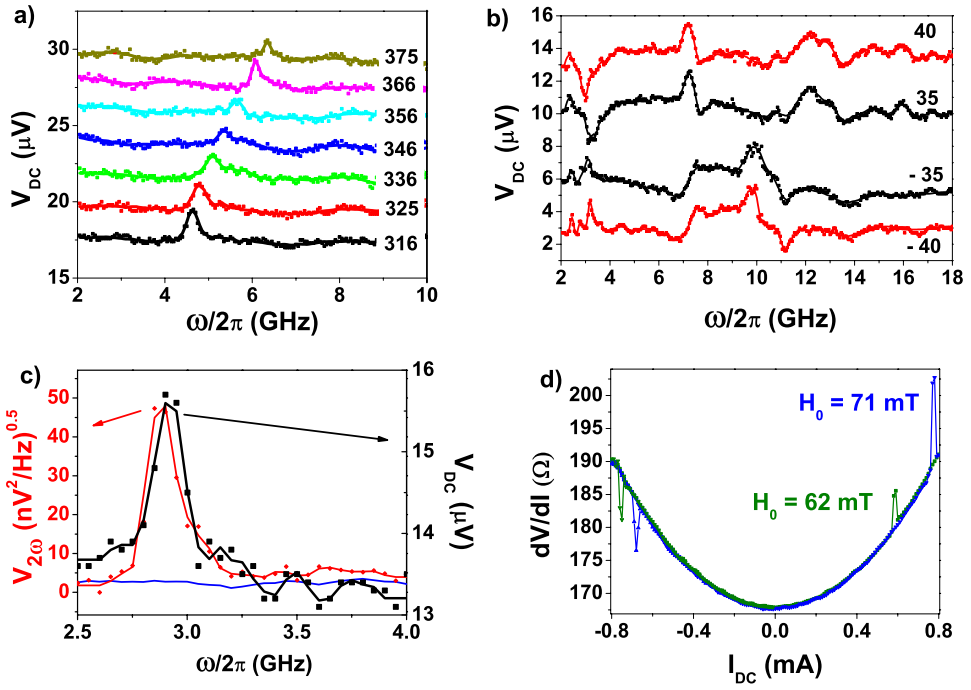


FIG. 2. (Color online) $V_{\text{dc}}$ (measured with a voltmeter) as a function of the ac frequency for (a) high and (b) low fields. The curves are shifted by 2 μV for clarity. Numbers on the figure correspond to the amplitude of the external field $H_0$ in mT. (c) Signal at twice the excitation frequency (red) and $V_{\text{dc}}$ (black) recorded simultaneously. The harmonic signal is measured with a spectrum analyzer. The baseline (blue) is recorded at saturation field. Measurements of the harmonic signals are averaged 1000 times to increase the signal-to-noise ratio. (d) $dV/dI$ as a function of $I_{\text{dc}}$ observed in a similar structure.

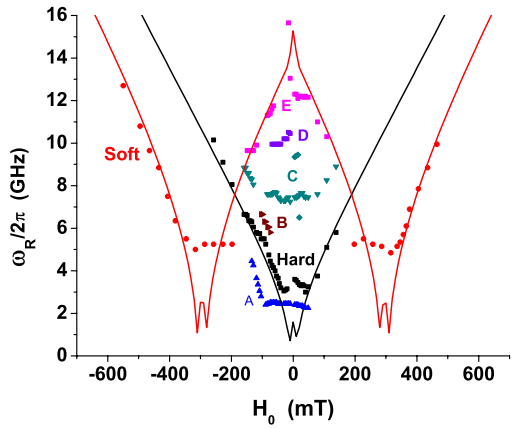


FIG. 3. (Color online) Evolution of the different resonant modes as a function of the applied field $H_0$. The red and black lines correspond to the fit with the macrospin model for the free and hard layers, respectively.

$$\frac{\omega_R}{2\pi} = \frac{\gamma}{M_S \sin(\theta_{\text{eq}})}\sqrt{F_{\theta\theta}F_{\varphi\varphi} - F_{\theta\varphi}^2}, \tag{1}$$

where $M_S$ is the layer magnetization at saturation, $\gamma$ is the gyromagnetic ratio (29 GHz/T), and $\theta_{\text{eq}}$ is the equilibrium angle between the magnetization and the normal to the spin valve plane. The second partial derivatives of the free energy $F$ are calculated at equilibrium position $\theta_{\text{eq}}$ and $\varphi_{\text{eq}}$ which is determined from the minimization of the free energy. For each layer, $F$ contains the Zeeman and the magnetostatic energies. The values of the different demagnetizing factors are calculated from Ref. 21. For the SL we add to $F$ a dipolar interaction with the HL.

The parameters necessary for our computation have been taken from previous studies realized in our group.[19] In particular, the cross section of the spin valve can be assumed to be slightly elliptical since the layers were found to be deposited with a small average angle ($<\pi/18$) with respect to the pore axis. Hence, the dimensions of the ellipse are 90 $\times 80$ nm$^2$. The value of $\mu_0 M_s$ is 1 T, in good agreement with our superconducting quantum interference device (SQUID) measurement.

The results of the calculation for each layer correspond to the red (SL) and black (HL) lines in Fig. 3. Whereas we observed a good agreement between the macrospin calculations and several experimental peaks, especially in the nearly saturated regime of each layer, we also observed a clear discrepancy between the macrospin model and the modes A–D in the field range corresponding to the plateau in the GMR. This result demonstrates the very complex spin dynamics behavior of such a nanoscale system, especially in the low-field range relevant for applications. Micromagnetic calculations would be necessary to achieve a deeper understanding of these modes, which most probably correspond to spatially nonuniform excitations. For example, micromagnetic calculations reported in Ref. 22 have shown numerous spatially nonuniform modes in a single elliptical nanomagnet. Notably, a microwave magnetic field with a poloidal symmetry has been shown to excite a nonuniform mode localized near the edge of the structure (see Fig. 1 in Ref. 22). This mode has been found to be a low energy mode. Hence, it may be that mode A observed in Fig. 3 is such a mode excited by the field induced by the microwave current passing through the nanowire. However, one can note that the magnetic field induced by the current does not present the appropriate spatial symmetry to excite uniform modes, which can only be excited by spin torque.

We observed that the field dependence of the frequency of modes A, B, and D is not symmetric to $H_0=0$. Since the dynamic modes depend on the equilibrium magnetic configurations, this asymmetry reflects the field shift of the magnetic hysteresis shown by the magnetoresistance (red curve in Fig. 1). Finally, the plateau in the $190<|H_0|<280$ mT field range observed for the mode denoted by red circles may arise from nonuniformity of the magnetization in the SL, which is expected at fields where $H_{\text{bias}}$, $H_0$, and the demagnetizing field compete. Interface roughness can also influence the magnetic configuration. These effects are well-known limitations of the macrospin approximation.

In summary, microwave currents were applied to a sub-100 nm spin valve, and both dc and second-harmonic signals were detected with good signal-to-noise ratios. Thanks to the flexibility of the template synthesis method, we were able to grow nanostructures and contact bump pads on a tiny holder fitted to a high-frequency connector. Thus, lithography processing was avoided throughout. We demonstrated that the ac excites the uniform oscillation of both magnetic layers in the near saturated regime, in agreement with STT theory. Higher order magnetic excitations were detected at low fields. These results are relevant to microwave oscillator applications and the method developed is promising for integrating multiple resonators in series.

This work was supported by the Swiss NSF Grant No. 200020-117588. The authors thank Michel Viret for helpful discussions.

[1] J. Slonczewski, J. Magn. Magn. Mater. **159**, L1 (1996).
[2] L. Berger, Phys. Rev. B **54**, 9353 (1996).
[3] M. Tsoi, A. G. M. Jansen, J. Bass, W. C. Chiang, V. Tsoi, and P. Wyder, Nature (London) **406**, 46 (2000).
[4] J. A. Katine, F. J. Albert, R. A. Buhrman, E. B. Myers, and D. C. Ralph, Phys. Rev. Lett. **84**, 3149 (2000).
[5] J. E. Wegrowe, D. Kelly, T. Truong, Ph. Guitienne, and J.-Ph. Ansermet, Europhys. Lett. **56**, 748 (2001).
[6] Yaomen Liu, Zongzhi Zhang, P. P. Freitas, and J. L. Martins, Appl. Phys. Lett. **82**, 2871 (2003).
[7] A. Deac, K. J. Lee, Y. Liu, O. Redon, M. Li, P. Wang, J. P. Nozieres, and B. Dieny, Phys. Rev. B **73**, 064414 (2006).
[8] S. I. Kiselev, J. C. Sankey, I. N. Krivorotov, N. C. Emley, R. J. Schoelkopf, R. A. Buhrman, and D. C. Ralph, Nature (London)

**425**, 380 (2003).
[9] M. R. Pufall, W. H. Rippard, S. E. Russek, S. Kaka, and J. A. Katine, Phys. Rev. Lett. **97**, 087206 (2006).
[10] A. A. Tulapurkar, Y. Suzuki, A. Fukushima, H. Kubota, H. Maehara, K. Tsunekawa, D. D. Djayaprawira, N. Watanabe, and S. Yuasa, Nature (London) **438**, 339 (2005).
[11] J. C. Sankey, P. M. Braganca, A. G. F. Garcia, I. N. Krivorotov, R. A. Buhrman, and D. C. Ralph, Phys. Rev. Lett. **96**, 227601 (2006).
[12] W. Chen, J. M. L. Beaujour, G. de Loubens, A. D. Kent, and J. Z. Sun, Appl. Phys. Lett. **92**, 012507 (2008).
[13] S. H. Florez, J. A. Katine, M. Carey, L. Folks, and B. D. Terris, J. Appl. Phys. **103**, 07A708 (2008).
[14] G. D. Fuchs, J. C. Sankey, V. S. Pribiag, L. Qian, P. M. Braganga, A. G. F. Garcia, E. M. Ryan, Z. P. Li, O. Ozatay, D. C. Ralph, and R. A. Burhman, Appl. Phys. Lett. **91**, 062507 (2007).
[15] C. R. Martin, Science **266**, 1961 (1994).
[16] W. Schwarzacher and D. S. Lashmore, IEEE Trans. Magn. **32**, 3133 (1996).
[17] L. Piraux, K. Renard, R. Guillemet, S. Matefli-Tempfli, M. Matefli-Tempfli, V. A. Antohe, S. Fusil, K. Bouzehouane, and V. Cros, Nano Lett. **7**, 2563 (2007).
[18] A. A. Kovalev, G. E. W. Bauer, and A. Brataas, Phys. Rev. B **75**, 014430 (2007).
[19] D. Doudin, A. Blondel, and J.-Ph. Ansermet, J. Appl. Phys. **79**, 6090 (1996); D. Doudin, J. E. Wegrowe, S. E. Gilbert, V. Scarani, D. Kelly, J. P. Meier, and J.-Ph. Ansermet, IEEE Trans. Magn. **34**, 968 (1998); B. Doudin and J.-Ph. Ansermet, Nanostruct. Mater. **6**, 521 (1995).
[20] S. D. Vonsovskii, *Ferromagnetic Resonance* (Pergamon, New York, 1966).
[21] J. A. Osborn, Phys. Rev. **67**, 351 (1945).
[22] R. D. McMichael and M. D. Stiles, J. Appl. Phys. **97**, 10J901 (2005).